Error Tracking in IKONOS Geometric Processing

Using a 3D Parametric Modelling

Tracking of input data error propagation during the 3D geometric processing

of IKONOS Geo-product images with a parametric modelling

ABSTRACT

Thirteen Pan or XS IKONOS Geo-product images over seven study sites with various environments and terrain were tested using different cartographic data and accuracies using a parametric modelling developed at the Canada Centre for Remote Sensing. The objectives were to define the relationship between the final accuracy, the number and accuracy of input data and to track the error propagation during the full geometric correction process (bundle adjustment and ortho-rectification) to finally advice on the applicability of the model in operational environments.

When ground control points (GCPs) are less than 3-m accurate, 20 GCPs over the full image is a good compromise to obtain 3-4 m accuracy in the bundle adjustment. When they are better than 1-m, 10 GCPs are then enough to increase to 2-3 m accuracy with either panchromatic or multiband images. Since GCP residuals reflect the input data errors (map and/or plotting) these errors did not propagate through the modelling.

Quantitative and qualitative evaluations of ortho-images were performed with either independent check points or digital vector files overlaid. Generally, the measured errors confirm the predicted errors or even were slightly better, and 2-4 m positioning accuracy is achieved for the ortho-images depending of the elevation accuracy (DEM

and grid spacing). To achieve a better final positioning accuracy, such as 1 m, 1-2 m accurate DEM with fine grid spacing is required in addition to the well-defined GCPs.

1 INTRODUCTION

The generation of high-resolution imagery using previously-proven defence technology provides an interesting source of data for digital topographic mapping as well as thematic applications such as agriculture, forestry, and emergency response (Kaufmann und Sulzer, 1997; Konecny, 1999). Technical informations on the new US civilian satellites with their future applicability to earth sciences have been summarized by Fritz (1996). Highly detailed maps of entire countries could be updated using this data. Farmers could monitor the health of their crops and estimate yields with greater accuracy and over shorter intervals. Scientists could look at environmentally sensitive areas and government officials could monitor and plan more enlightened land use policies. City planners could further plan the development of new housing communities with greater precision and attention.

IKONOS, the first commercial satellite with the highest publicly available resolution, which was successfully launched September 24 1999, can fill these requirements. The satellite's sensor generate 1-m panchromatic (Pan) and 4-m multiband (XS) images with off-nadir viewing up-to-60º in any azimuth (Space Imaging, 2001). The principal attraction for the user community is the 1-m pixel, which enables the extraction of objects appearing in most digital mapping products. The off-nadir viewing capability is also an important characteristic since it improves the revisit rate of the same ground area to between two and three days, and also enables the acquisition of stereo-images. Users could then apply traditional photogrammetric techniques with these stereo-images to extract planimetric and altimetric information.

In order to be prepared to the appropriate use of this new source of data, different research studies have addressed the potential of high-resolution imagery for mapping. A first research study at the National Mapping Agency of Great Britain used simulated 0.2-m and 1-m Pan images derived from 1:7,500-scale aerial photos and XS 4-m images from the Compact Airborne Spectrographic Images (CASI) (Ridley *et al.*, 1997). Some of results indicated that high-resolution satellite imagery would have potential for improving the existing National Topographic Database of Great Britain from 1-m panchromatic images as well as for automatically detecting topographic feature change from 4-m XS images. On the other hand, a theoretical analysis based on in-track and across-track stereo-mapping techniques demonstrated that high-resolution satellite imagery can be used for the generation and updating of national mapping products in the United States, only if strict photogrammetric processing are employed (Li, 1998). Based on this theoretical analysis, an evaluation of the potential accuracy of ground points has been performed using IKONOS stereo-images simulated from aerial photos (Zhou and Li, 2000). Ground point accuracy of 12 m in the three axes (X, Y and Z) was achieved without ground control points (GCPs), but with 24 GCPs an accuracy of 3 m in planimetry (X and Y) and 2 m in elevation was obtained. More recently, preliminary accuracy tests with real images (viewing angle of 39º) using a parametric geometric correction model were performed with 7 or 10 precise GCPs (Toutin and Cheng, 2000; Davies and Wang, 2001). Their results demonstrated accuracy in planimetry of around 2-3 m and then confirmed that IKONOS images have a high potential for mapping.

The objectives of this paper are to expand on these preliminary results with a larger data set of IKONOS images: 1-m Pan and 4-m XS, acquired with 10º-30º viewing angles at different azimuth angles. The study sites span low-to-high relief in urban, semi-rural and rural areas of North America and Europe with different topographic data and accuracy. Using a multi-sensor geometric model developed at the Canada Centre for Remote Sensing (CCRS) (Toutin, 1995) and adapted to IKONOS images (Toutin and

Cheng, 2000), the paper will track the error propagation from the input data to the final ortho-image. Different cartographic parameters affecting the accuracy, such as the definition, number, location and accuracy of GCPs and the accuracy and grid spacing of digital elevation model (DEM) are also evaluated. Finally, future research studies and advises for operational uses are given as a function of these results.

1 IKONOS Data and Processing

IKONOS orbits the Earth once every 98 minutes at an altitude of approximately 680 kilometres. Since it is in a sun-synchronous orbit it passes a given latitude at about the same local time each day. The satellite orbit exactly repeats every 140 days. However, since the sensor is capable of viewing up-to-60º in any azimuth (in-track and cross-track pointing), a site can be imaged almost daily, although not always at one-meter resolution. The satellite's sensor generates 1-m Pan and 4-m XS images if they are acquired with a viewing angle between 0º and 26º. Over 26º viewing angles Space Imaging insures 2-m resolution for the panchromatic images (Space Imaging, 2001).

In some of the previous studies, IKONOS simulations generated raw image products in order to apply strict photogrammetric processing (Li, 1998; Zhou and Li, 2000). Unfortunately, raw image products are not available to end-users. Only map georeferenced and a range of orthorectified products with applied geometric correction and oriented to the North are delivered by Space Imaging. These products meet U.S. National Map Accuracy Standards (NMAS) for scales between 1:100,000 and 1:2,400. Table 1 shows an example of the basic panchromatic products. The data is distributed in 8-bit or 11-bit GeoTiff format with ASCII metadata file, including order parameters and also source image and products file descriptions. Following confirmation, delivery of orders that are available from archive typically takes several days to just over a week. Delivery of newly collected data typically takes 60 days, depending upon order size, weather, accuracy, and both GCPs and DEM acquisition time.

The Geo product, which is the most affordable but offers the lowest positioning accuracy, is not corrected for terrain distortions. It has an accuracy of 50m CE90, which means that any point within the image is within 50 meters horizontally of its true position on the Earth's surface 90% of the time. Accuracy becomes worse in mountainous areas if the images are acquired with off-nadir viewing, which is quite common for the IKONOS data. In fact, the estimated horizontal accuracy given in the metadata of one mountainous study site was between 300 m and 1000 m. Hence, the product will only meet the geometric requirements of mapping scale at 1:250,000 in flat area or less in mountainous areas.

The Precision Plus product is the most expensive but offers the highest positioning accuracy (2 m CE90). To achieve it, Space Imaging will generally acquire GCP for both domestic and international orders at no additional charge. At its sole discretion, Space Imaging may require customer to provide ground control. However, because most of the images are acquired at off-nadir viewing, the accuracy of GCPs and DEM should be within 1 m and 5 m, respectively.

Even though detailed sensor information for the IKONOS satellite is not released, a rigorous IKONOS model using basic information from the metadata and image files has been developed (Toutin and Cheng, 2000). The IKONOS model is based upon a previous parametric model developed for multi-sensor images (Toutin, 1995). It has been applied with 3 to 6 GCPs to VIR data (Landsat 5 & 7, SPOT, IRS, ASTER, and KOMPSAT), as well as radar data (ERS, JERS, SIR-C and RADARSAT). Based on good quality GCPs, the accuracy of this model was proven to be within one-third of a pixel for medium-resolution images, two pixels for high-resolution IKONOS images and one resolution cell for radar images. Since the geometric processing steps of the IKONOS images are roughly the same than for the other images (data collection, bundle adjustment and ortho-rectification), more details on the method and the processing steps

can be found in Toutin (1995). The paper then concentrates on the error propagation of the input data along the processing steps and the accuracy evaluation is performed during the two main processing steps:

(1) On independent check points (ICPs) during the computation of the bundle adjustment with different numbers and accuracy of GCPs;
(2) By overlaying digital vector data or by comparing with ICPs on the ortho-images generated with DEM.

2 STUDY SITES and DATA SET

Seven study sites with different environments and relief are used in this research study (Table 2):

1. Toronto, Ontario, Canada is a sub-urban environment and a flat topography with 60-m elevation range;
2. Beauport, Quebec, Canada is a residential and semi-rural environment and a hilly topography with 500-m elevation range;
3. Toulouse, France is an sub-urban environment and a flat topography with 100-m elevation range;
4. Trier, Germany is an urban and semi-rural environment and a rolling topography with 300-m elevation range;
5. Dresden, Germany is a rural environment and a rolling topography with 300-m elevation range (Meinel *et al.*, 2001);
6. Caracas, Venezuela is a urban and rural environment and a mountainous topography with 2200-m elevation range (Arismendi *et al.*, 2000); and
7. Luzern, Switzerland is an urban and rural environment and a mountainous topography with 2000-m elevation range.

For each site IKONOS Geo-product data, covering an area of approximately 10 km by

10 km, have been acquired either in Pan mode (1-m pixel spacing) and/or XS mode (4-m pixel spacing):

1. For Toronto, Ontario, Canada, a Pan image acquired April 23, 2000 with collection and azimuth angles of 51º and 21º, respectively;
2. For Beauport, Quebec, Canada, two Pan images acquired January 3, 2001 with collection and azimuth angles for each image of 63º and 322º, 63º and 252º, respectively;
3. Toulouse, France, Pan and XS images simultaneously acquired May 14, 2000 with collection and azimuth angles of 70º and 138º, respectively;
4. Trier, Germany, a XS image acquired June 13, 2000 with collection and azimuth angles of 65º and 177º, respectively;
5. Dresden, Germany, Pan and XS co-registred images simultaneously acquired August 1, 2000 with collection and azimuth angles of 71º and 335º, respectively;
6. Caracas, Venezuela, four Pan in-track images acquired form the same orbit December 30, 1999 with collection and azimuth angles for each image of 59º and 12º, 65º and 46º, 73º and 71º, 76º and 122º, respectively; and
7. Luzern, Switzerland, a Pan image acquired April 22, 2000 with collection and azimuth angles of 68º and 256º, respectively.

The cartographic data, some acquired by international collaborators, are:

1. For Toronto, Ontario, Canada, 30 GCPs were collected and their map coordinates were obtained from 20-cm pixel ortho-photos with 0.5-m accuracy and 2-m grid spacing DEM with 5-m accuracy;
2. For Beauport, Quebec, Canada, 56 GCPs were collected and their map coordinates were obtained from six 1-m pixel ortho-photos with 3-m accuracy and 5-m grid spacing DEM with 5-m accuracy. However, a mean positioning error of 5-7 m in the X direction was found between the different ortho-photos; this error is mainly due to 5-m DEM error during the ortho-photo generation;
3. For Toulouse, France, 33 GCPs were collected and their map coordinates were

obtained from 0.5-m pixel ortho-photo mosaic with 1-m accuracy and 10-m grid spacing DEM with 5-m accuracy;

4. For Trier, Germany, 23 GCPs were collected and their map coordinates were obtained from differential GPS with 0.5-m accuracy and 20-m grid spacing DEM with 5-m accuracy;
5. For Dresden, Germany, 112 GCPs were collected and their map coordinates were obtained from 1:10,000 topographic maps with 4-m accuracy and 1-m grid spacing laserscanning DEM with 1-m accuracy. In addition, a second set of map coordinates (118 GCPs) were obtained from 0.4-m pixel ortho-photo mosaic with 1-m accuracy;
6. For Caracas, Venezuela, around 30 GCPs were collected for each image and their map coordinates were obtained from 2.5-m pixel ortho-photos with 5-m accuracy and 5-m grid spacing DEM with 5-m accuracy; and
7. For Luzern, Switzerland, 70 GCPs were collected and their map coordinates were obtained from 1.25-m pixel images of scanned 1:25,000 topographic maps with 5-m accuracy in the three axes.

Since the processing is performed on the full image area, GCPs cover the total surface (100 km^2) with also points at the lowest and highest elevation to avoid extrapolations, both in planimetry and altimetry. In general, the plotting accuracy for Pan images is about 1-2 pixels in the urban and sub-urban areas and 2-3 pixels in the rural and mountainous areas due to the difficulty to find and locate 1-m precise ground elements. For XS images, the plotting accuracy depends of the method used to evaluate different possibilities and the environment:

- in the Trier site, GCPs have been plotted on the XS image, most of them in the urban environment with an accuracy of half-pixel (about 2 m);
- in the Dresden site, GCP coordinates have been imported and computed by dividing by four from Pan image coordinates with the same accuracy, 2-3 m in rural environment; and

- in the Toulouse site, GCPs collected on the Pan image have been re-plotted on the XS image with an accuracy better than one pixel. However, these points are not necessarily the best defined in the XS image.

3 RESULTS AND DISCUSSIONS

The error propagation can be tracked along the geometric processing steps with bundle adjustment results as a function of GCP numbers, location and accuracies and with the ortho-images as a function of DEM accuracy and spacing. It should be noted that the processing is performed on the full image size (about 100 km^2) and not only on small sub-area.

Bundle Adjustment Results

The first test is performed using all the GCPs in the bundle adjustment of each image. Table 3 summarizes these results with the residuals on GCPs. With the parametric modelling, the residuals do not reflect the modelling accuracy but the error of the input data when there are more GCPs than the minimum required (Toutin, 1995). In fact, the first analysis demonstrates that the root mean square (RMS) residuals are generally in the same order of magnitude than the GCP planimetric error (plotting and map), in addition with the propagation of GCP Z-error depending of collection and azimuth angles.

With the Beauport site, the GCP RMS residual is larger in X (5.8 m) than in Y (2.2 m), such as the map X-error was found to be larger (5-7 m) than the Y-error (3 m). With the Toulouse site, the residuals relatively to pixel spacing are slightly worse with the Pan image than with the XS image, due to the GCP collection in the XS image. With the Dresden site, the residuals are better with the good GCP coordinates data set (1 versus 2). With mountainous Luzern site, the propagation of GCP Z-error (around 2-3 m) is

principally included in the X direction (collection and azimuth angles of 68º and 256º, respectively), which explain the larger RMS residual in X than in Y.

Refining this first analysis demonstrates that the RMS residuals are slightly larger than the GCP planimetric error when the input coordinates are 1-m or less precise (Toronto, Toulouse, Trier, Dresden_2). It is the reverse when the input coordinates are 5-m precise (Beauport, Dresden_1, Caracas, Luzern). In fact, the plotting error is the major source of error in the first case (2-3 m versus 1 m) while the map coordinate error is the major source in the second case (5 m versus 2-3 m). When the plotting error is the major source of error, it thus explains that:

- the RMS residual differences between Pan and XS images (Toulouse) are not proportional to pixel spacing because the plotting accuracy is about the same (2-3 m);
- the RMS residuals in urban environment (Toronto, Trier) are better than the RMS residuals in rural environment (Toulouse, Dresden_2) because the GCP definition and plotting are more accurate in urban environment; and
- The RMS residuals for XS images are correlated with the plotting error: the best results for Trier (RMS and plotting error of 1.4 m and 2 m, respectively) and the worse for Toulouse (RMS and plotting error of 3 m and 4 m, respectively). In Toulouse the GCPs firstly collected from the Pan image were not necessarily the best-defined points in the XS image.

The second analysis is that the X-Y minimum/maximum residuals are generally around two and sometimes three times the RMS residuals. It demonstrates stability over the entire images without generating local errors. The use of overabundant GCPs (6 is the theoretical minimum) in the least square bundle adjustment has reduced the propagation of the different input data errors (plotting and/or map) in the modelling, but conversely these input errors are reflected in the residuals.

However, unbiased validation of the positioning accuracy has to be realized with ICPs, which are not used in the parametric model calculation. Different GCPs/ICPs configurations using the Dresden site, which has the most complete data set, were thus evaluated to find the optimal number of GCPs in relation with the error of the cartographic co-ordinates. With Dresden_Pan1 data set, the number of GCPs varies from 112 to 6 and the results (Figure 1) are evaluated on the 118 1-m accurate ICPs from the second set of coordinates (Dresden_Pan2). With Dresden_Pan2 data set, the number of GCPs varies from 70 to 6 and the results (Figure 2) are evaluated on the remaining ICPs (from 48 to 112, respectively).

In Figure 1, the RMS error on ICPs is always more than 3 m whatever the number of GCPs (even 112), and 15-20 GCPs are a good compromise to keep 3-4 m accuracy. The combination of cartographic and plotting errors (4 m and 2-3 m, respectively) avoid a better accuracy to be obtained, even with a large degree of freedom in the least square adjustment. On the other hand (Figure 2), the RMS error consistently decreases to 2-3 m when using the 1-m accurate second set of GCP coordinates (Dresden_Pan2), with slightly better results in the Y-coordinate. Ten precisely located GCPs are then a good compromise to achieve this 2-3 m accuracy. For this test, the RMS error reflects the major source of error, which is the plotting error (2-3 m).

By applying these values (25 GCPs for 5-m accurate coordinates and 10 GCPs for 1-m accurate coordinates) on the other data set, Table 4 shows statistical results of the bundle adjustment: number of GCPs/ICPs and the RMS and minimum/maximum errors on the ICPs. For some data sets (Toronto, Caracas), a smaller number of GCPs is used to keep enough ICPs for the statistical evaluation. When the cartographic coordinates are 1-m precise (Toronto, Toulouse, Trier, Dresden_2), RMS errors are always around 2-3 m with slightly worse results for Toulouse. The accuracies for these data sets are due to the plotting errors for each image depending of the environment. When the cartographic coordinates are 5-m precise (Beauport, Dresden_1, Caracas, Luzern), the

RMS errors are a little worse than 3-5 m with slightly worse results for Beauport in the X-direction due to the ortho-photo X-error. The slightly worse results for Caracas are partly related to the reduced number of GCPs in the least square adjustment: 12 instead of 20 reducing the advantages of least square adjustment. Consequently, the errors for these data sets result from the map coordinate errors for each study site. These full results then confirm the preliminary results on Dresden. Finally, the RMS errors on ICPs are about the same (10-15% higher) than the RMS residuals on GCPs (Tables 3) and are in the order of magnitude of the input data errors. Most of the comments and explanations given for Table 3 results then applied for Table 4 results: e.g., the results of the bundle adjustment reflect the cartographic error and these cartographic error does not propagate through the modelling but through the residuals.

The last test on bundle adjustment is related to the location of GCPs. It is well known that extrapolation in planimetry outside of the GCP boundary is not recommended. However, it is not well recognized that large extrapolation should also not be applied in the elevation direction. To test the impact of elevation extrapolation, Caracas and Luzern study sites are used because they have more than 2000-m elevation difference. When the highest GCP used in the bundle adjustment is 1000-m lower than the mountain summit (generating 1000-m extrapolation) the largest planimetric errors on the highest ICPs are around 20-30 m. This error reduced to 10 m when the elevation extrapolation is reduced to 500 m.

These three tests demonstrate that the CCRS-developed model and method are both stable and robust for IKONOS Geo-product images without generating local errors, and filter random or systematic errors. The input GCP error does not propagate through the rigorous model, but is reflected in the residual. Since GCP residuals are on the same order of magnitude than ICPs errors they can thus be used as *a priori* mapping error in operational environments, only taking into account the cartographic data errors. It then gives a good level of confidence of the applicability and robustness of the CCRS parametric model applied to IKONOS Geo-product data in operational environments.

Ortho-images Results

Ortho-images have been generated in the conformal cartographic projection system of the user for four different data sets (Beauport_A, Trier, Dresden and Caracas). These sites were chosen because digital vector files were available with 1-3 m accuracy depending of the study site. The ortho-correction process uses the parameters of the geometric model previously determined in the least-square bundle adjustment. Since the geometric model takes into account the elevation distortion, elevation information is needed to create precise ortho-images. Elevations generally extracted from DEM have errors, which propagate through the rectification process in addition to the previous errors of the bundle adjustment process. The elevation errors for the data sets are mainly dominated by two sources: the error on the elevation at the DEM grid point and the error due to the linear interpolation between grid points depending of the terrain slopes. Let use two examples. For Trier, 20-m grid spacing DEM with 5-m accuracy and a rolling relief with slopes less than 10º generate an elevation error of about 5 m. For Caracas, 5-m grid spacing DEM with 5-m accuracy and a mountainous relief with slopes less than 45º generate an elevation error of about 6 m.

To compute the propagation of the elevation errors into the ortho-image as a function of the viewing angle, curves (Figure 3) mathematically computed with the elevation distortion parameters of the geometric modelling are used (Toutin, 1995). Consequently for Trier and Caracas_A images acquired with viewing angles of 25º and 31º, the 5-m and 6-m elevation errors generate planimetric errors on the ortho-images of about 2 m and 4 m, respectively. Inversely, if a 1-m planimetric accuracy for the ortho-image is required with a 30º-viewing angle (normally acquired by Space Imaging), the elevation should have an error of 1.5-2 m. Finally, the predicted final circular error of the ortho-images, as a combination of the bundle adjustment errors (Table 4) and the elevation error propagation, is about 4 m and 6 m for Trier and Caracas_A, respectively.

To confirm these predicted evaluations, a qualitative and visual evaluation of the ortho-images for the four study sites are performed. For Beauport_A, a first quantitative comparison of the panchromatic ortho-image (1-m pixel) was realized with 31 independent check points extracted both from 3-m accurate vector lines. RMS errors of 5 m and 3 m with 1.5-m and –0.5-m bias for X and Y, respectively were computed with no errors larger than 10 m when compared to the vector lines. In a second step to perform a qualitative analysis, the vector lines are overlaid on the ortho-image (Figure 4, top) and the ortho-photo (Figure 4, bottom). The road vector lines are always inside the IKONOS roads: considering 10-m width for the main road, 4-m error can be estimated. These two estimated errors from checkpoints and vector lines are better than a circular error of 8 m directly computed from the ICP errors (Table 4) (the 5-m elevation error has only 2.5-m error impact in the error budget). However, the 5-7 m X-error of the ortho-photos is included in the 8-m circular error, which then biased the predicted error. Furthermore, when comparing the same roads overlaid on the 1-m ortho-photo the same deviations can be noticed: it could mean that part of errors comes from the 3-m error vector lines. Evaluation on other features, such as secondary roads, rivers and even private houses confirms the 4-m error.

For Dresden, the quantitative comparison of the Pan ortho-image (1-m pixel) was independently realized at Dresden using 31 independent check points extracted from the 0.4-m pixel ortho-photo mosaic with 1-m accuracy. RMS errors of 2 m with 0.5-m bias in both axes were computed with no errors larger than 5 m. It is consistent with a circular error of 3 m directly computed from the ICP errors (Table 4) because the 1-m elevation error has a minor impact in the ortho-rectification process and in the error budget.

Figure 5 shows two sub-areas of the ortho-images: the XS (2-m pixel) of Trier at the top and the Pan (1-m pixel) of Dresden at the bottom with vector files from the German topographic data base with an accuracy of 2 m. Both images with the vector files were

evaluated both in Canada and Germany: there is in general a good superposition between the vectors on the appropriate image features. The Trier sub-area (640 pixels by 440 lines) is the most pronounced relief area of the full image with 150-m elevation variation along a steep vineyard. The cartographic lines along the slope, such as in the villages appear to exactly conform to ortho-image geometry with one pixel error (2 m). It is more evident in 3-m wide vineyard tracks. This approximate error evaluation is consistent and even better than the predicted error of 4 m, previously computed. For Dresden sub-area (940 pixels by 660 lines), the coastlines of the river show errors no more than 2-3 pixels (2-3 m). Other well defined features, such as roads or city streets visually show the same accurate superposition with the ortho-image in accordance with the check point accuracy evaluation previously done.

Since four Caracas images are available with some overlaps, 1-m pixel ortho-mosaic were realized. Relative and absolute evaluations are then performed on two areas of the ortho-mosaic: in an overlap area of Caracas_A and B images in the mountains (Figure 6), and in a coastal area with the 1:1,000 2-m accurate vector lines overlaid (Figure 7). The radiometric variations between the two images of Figure 6 were increased to show the seed of the mosaic. The relative accuracy between the images can be thus evaluated on three mountain roads at the seed. It is in the order of 2 m with a maximum error of 6 m for the lowest mountain road. The 1:1,000 vector lines displayed in Figure 7 show many details not visible on the IKONOS ortho-image for defining a superposition error. However, using the vectors representing the edge of 5-m wide largest roads, an absolute accuracy can be approximated to be 3-4 m with maximum error less than 10 m: it is more obvious with the sport field on the left. It thus confirms the predicted evaluation of 6 m.

4 CONCLUSION

To expand on the applicability of CCRS-developed geometric model for IKONOS Geo-product images, 13 Pan or XS images from five international collaborators over seven study sites with various environments and terrain were tested. Cartographic data (maps, ortho-photos, GCPs, DEM, digital vector files) were acquired from different sources, methods and accuracy. The objective of the paper was to define the relationship between the final accuracy, the number and accuracy of input data (GCPs and DEM). Consequently, a secondary objective was to track the error propagation during the full geometric correction process (bundle adjustment and ortho-rectification) to finally advice on the applicability of the model in operational environments.

When GCPs are less than 3-m accurate, 20 GCPs is a good compromise to obtain 3-4 m accuracy in the bundle adjustment. When they are better than 1-m, 10 GCPs are then enough to achieve 2-3 m accuracy. In the first result, map coordinates is the major source of error while it is the GCP definition and plotting error in the second result. The relationship between the plotting error and the residuals was also noticed with the three different GCP collection methods of XS images. During the least square adjustment of a parametric modelling the errors of the input data do not thus propagates in the model, but in the residuals. Since residuals reflect the input data error, it is thus normal and "safe" to obtain 5-10 m residuals if the GCPs are only 10-m accurate, but it does not mean that the geometric modelling will be only 5-10-m precise. With good GCPs (1-2 pixel accurate for the definition and plotting; 1-m accurate for the map coordinates), 2-m accuracy can be achieved in the bundle adjustment of both Pan and XS images (Toronto and Trier, respectively). Since definition and plotting error of GCPs becomes a key aspect with IKONOS images to increase the final accuracy (to 1-2 m), future research at CCRS will address this point with benchmark on the ground for defining 1-m precise GCP, as it was traditionally done in photogrammetry.

To track the error during the ortho-rectification, an evaluation of elevation errors were done as a function of DEM accuracy and grid spacing and the terrain relief with its

impact on the ortho-image as a function of the viewing angle. By combining it with the bundle adjustment errors, predicted accuracy was then computed for different study sites: it then enables the users to better manage each error in the error budget. Quantitative and qualitative evaluations of relative and absolute errors in the ortho-images were performed with either independent check points or digital vector files overlaid. Generally, the measured errors confirm the predicted errors or even were slightly better: 2-m accuracy was achieved for some ortho-images when the cartographic data was of good quality and 4-m accuracy for the others. To achieve a better positioning accuracy, such as 1 m, 1-2 m accurate DEM with fine grid spacing is required in addition to precise GCPs (definition, plotting and map).

Acknowledgements

The author wants to thank his international collaborators for the IKONOS and/or cartographic data in the different study sites: Dr. Philip Cheng of PCI Geomatics, Canada for Toronto; Mr. Réjean Matte of Ministère des Ressources naturelles du Québec, Canada for Beauport; Mr. Didier Giacobbo of GDTA, France for Toulouse; Prof. Joachim Hill of Trier University, Germany, for Trier; Dr. Gotthard Meinel of Institut für ökologische Raumentwicklung, Germany for Dresden; Lic. Ramiro Salcedo of Instituto de Ingenieria, Venezula for Caracas; Mr. Jean-Pierre Perret of the Federal Office of Topography, Switzerland for Luzern. He also thanks MM. René Chénier and Yves Carbonneau of Consultants TGIS inc., Canada for the data processing.

References

Arismendi, J., R. Salcedo, y D. Varela, 2000, “Geomorfologia Actual y Cobertura Natural de la Vertiente Norte de la Cordillera de la Costa Afectada por el Evento

Hidrometeorologico de Diciembre 99, A Partir de la Interpretacion de Imagenes de Satelite", Proceedings of *IX International Symposium of the LatinAmerican Society of Remote Sensing (SELPER),* Puerto Iguazu, Misiones, Argentina, 6-10 Novembre 2000, pp. 505-516.

Davies C. H., and X. Wang, 2001, Planimetric Accuracy of IKONOS 1-m Panchromatic Image Products, *Proceedings of the 2001 ASPRS Annual Conference*, St. Louis, MI, USA, April 23 - 27, CD-ROM.

Fritz, L. W., 1996, The Era of Commercial Earth Observation Satellites. *Photogrammetric Engineering and Remote Sensing*, 62(1):39-45.

Kaufmann, V., und W. Sulzer, 1997, Über die Nutzungsmöglichkeit hochauflösender amerikanischer Spionage-Satellitenbilder (1960-1972), *Vermessung und Geoinformation*, Heft 3/97:166-173.

Konecny G., 2000, Mapping from Space, *Remote Sensing for Environmental Data in Albania: A Strategy for Integrated Management*, NATO Science Series, Vol. 72, Kluver Academic Publishers, pp. 41-58.

Li, R., 1998, Potential of High-Resolution Satellite Imagery for National Mapping Products. *Photogrammetric Engineering and Remote Sensing g*, 64(12):1165-1170.

Meinel, G., M. Neubert and J. Reder, 2001, Pixelorientierte versus segmentorientierte Klassification von IKONOS-Satellitenbildendaten – ein Methodenvergleich. *Photogrammetrie Fernerkundung Geoinformation*, Heft 3:157-170.

Ridley, H. M., P. M. Atkinson, P. Aplin, J.-P. Muller and I. Dowman 1997, Evaluating the Potential of the Forthcoming Commercial U.S. High-Resolution Satellite Sensor Imagery at the Ordnance Survey®. *Photogrammetric Engineering and Remote Sensing*, 63(8):997-1005.

Space Imaging, 2001, *www.spaceimaging.com*.

Toutin, Th., and P. Cheng, 2000, Demystification of IKONOS. *Earth Observation Magazine*, 9(7):17-21. http://www.ccrs.nrcan.gc.ca/ccrs/eduref/ref/bibpdf/4807.pdf.

Toutin, Th., 1995, Multisource data fusion with an integrated and unified geometric modelelling. *EARSeL Journal Advances in Remote Sensing*, 4(2):118-129. http://www.ccrs.nrcan.gc.ca/ccrs/eduref/ref/bibpdf/1223.pdf.

Zhou, G., and R. Li, 2000, Accuracy Evaluation of Ground Points from IKONOS High-Resolution Satellite Imagery. *Photogrammetric Engineering and Remote Sensing*, 66(9):1103-1112.

LIST OF FIGURES

LIST OF TABLES

Table 1: Detailed prices for basic panchromatic product from Space Imaging Web Site (http://www.spaceimaging.com/).

Product	**CE90**	**NMAS**
Geo	50 m	1:100,000
Reference	25 m	1:50,000
Pro	10 m	1:12,000
Precision	6 m	1:7,000
Precision Plus	2 m	1:2,400

Note: CE90 is the circular positioning accuracy with a confidence level of 90%. NMAS is the National Map Accuracy Standard in USA.

Table 2: Description of study sites with their description with environment, relief and elevation variation (Δelevation), of IKONOS images with mode, collection (Coll.) and azimuth (Az.) angles and of cartographic data with number of GCPs, accuracy of the planimetry (Plani.) and DEM. For Dresden study site, different GCPs were collected twice with different cartographic accuracies.

Study Site	Environment Type	Relief Δelevation	IKONOS Image			Cartographic Data		
			Mode	Coll.	Az.	GCP	Plani.	DEM
Toronto Canada	Sub-urban	Flat 60 m	Pan	51º	21º	30	0.5 m	5 m
Beauport Canada	Residential Semi-rural	Hilly 500 m	Pan Pan	63º 63º	322º 252º	55	3-7 m	5 m
Toulouse France	Sub-urban Rural	Flat 100 m	Pan XS	70º	138º	33	1 m	5 m
Trier Germany	Urban Semi-rural	Rolling 300 m	XS	65º	177º	23	0.5 m	5 m
Dresden Germany	Rural	Rolling 300 m	Pan XS	71º	335º	115	1) 4 m 2) 1 m	1 m
Caracas Venezuela	Urban Rural	Mountains 2200 m	4 Pan	59º to 76º	12º to 122º	30	5 m	5 m
Luzern Switzerland	Urban Rural	Mountains 1800 m	Pan	68º	256º	35	5 m	

Table 3: Bundle adjustment results for all study sites with the number and accuracy (in planimetry and elevation) of GCPs, the root mean square (RMS) and min./max residuals (in metres) on the GCPs. For Dresden study site, there are two sets of results as a function of different GCP numbers and accuracies. For Beauport and Caracas study site, results are given for the different Pan images (A, B, C, D).

Study Site	GCP Number	GCP Accuracy	RMS Residuals		Min./Max Residuals	
			X	Y	X	Y
Toronto	30	0.5 m, 1 m	0.8	1.1	-1/2	-3/2
Beauport_A	56	3-7 m, 5 m	5.8	2.2	-10/11	-5/5
Beauport_B	56	3-7 m, 5 m	6.0	2.1	-11/12	-5/5
Toulouse_Pan	33	1 m, 5 m	2.9	1.7	-5/7	-3/4
Toulouse_XS	33	1 m, 5 m	3.3	2.5	-7/7	-5/4
Trier	22	0.5 m, 5 m	1.4	1.4	-3/4	-2/3
Dresden_Pan1	112	4 m, 1 m	5.1	5.6	-13/12	-18/17
Dresden_XS1	112	4 m, 1 m	5.1	5.6	-13/12	-18/17
Dresden_Pan2	118	1 m, 1 m	2.3	1.6	-5/6	-4/5
Dresden_XS2	118	1 m, 1 m	2.3	1.6	-5/6	-4/5
Caracas_A	27	5 m, 5 m	2.7	3.4	-6/4	-6/7
Caracas_B	35	5 m, 5 m	5.3	5.3	-11/12	-9/14
Caracas_C	38	5 m, 5 m	5.1	2.2	-13/8	-4/4
Caracas_D	24	5 m, 5 m	2.8	4.1	-5/5	-9/7
Luzern	76	5 m, 5 m	5.6	2.8	-12/11	-8/5

Table 4: Bundle adjustment results for all study sites with the number of GCPs and ICPs, the root mean square (RMS) and min./max errors (in metres) on the ICPs. For Dresden study site, there are two sets of results as a function of different GCP numbers and accuracies. For Beauport and Caracas study sites, results are given for the different Pan images (A, B, C, D).

Study Site	GCP Number	ICP Number	RMS Errors		Min./Max Errors	
			X	Y	X	Y
Toronto	7	23	1.3	1.3	-3/3	-3/2
Beauport_A	20	36	7.5	2.7	-16/6	-2/6
Beauport_B	20	36	7.6	2.6	-16/11	-4/7
Toulouse_Pan	10	23	3.9	1.8	-8/3	-3/5
Toulouse_XS	10	23	4.9	3.3	-5/11	-6/5
Trier	10	12	2.3	1.8	-3/5	-2/4
Dresden_Pan1	20	118	4.1	2.7	-8/4	-5/8
Dresden_XS1	20	118	4.1	2.7	-8/4	-5/8
Dresden_Pan2	10	108	2.9	1.7	-7/7	-4/5
Dresden_XS2	10	108	2.9	1.7	-7/7	-4/5
Caracas_A	12	15	2.9	3.9	-6/4	-6/7
Caracas_B	12	23	6.4	4.4	-11/12	-9/14
Caracas_C	12	26	6.9	4.4	-13/8	-4/4
Caracas_D	12	12	3.4	4.4	-5/5	-9/7
Luzern	20	56	5.8	3.0	-10/11	-8/9

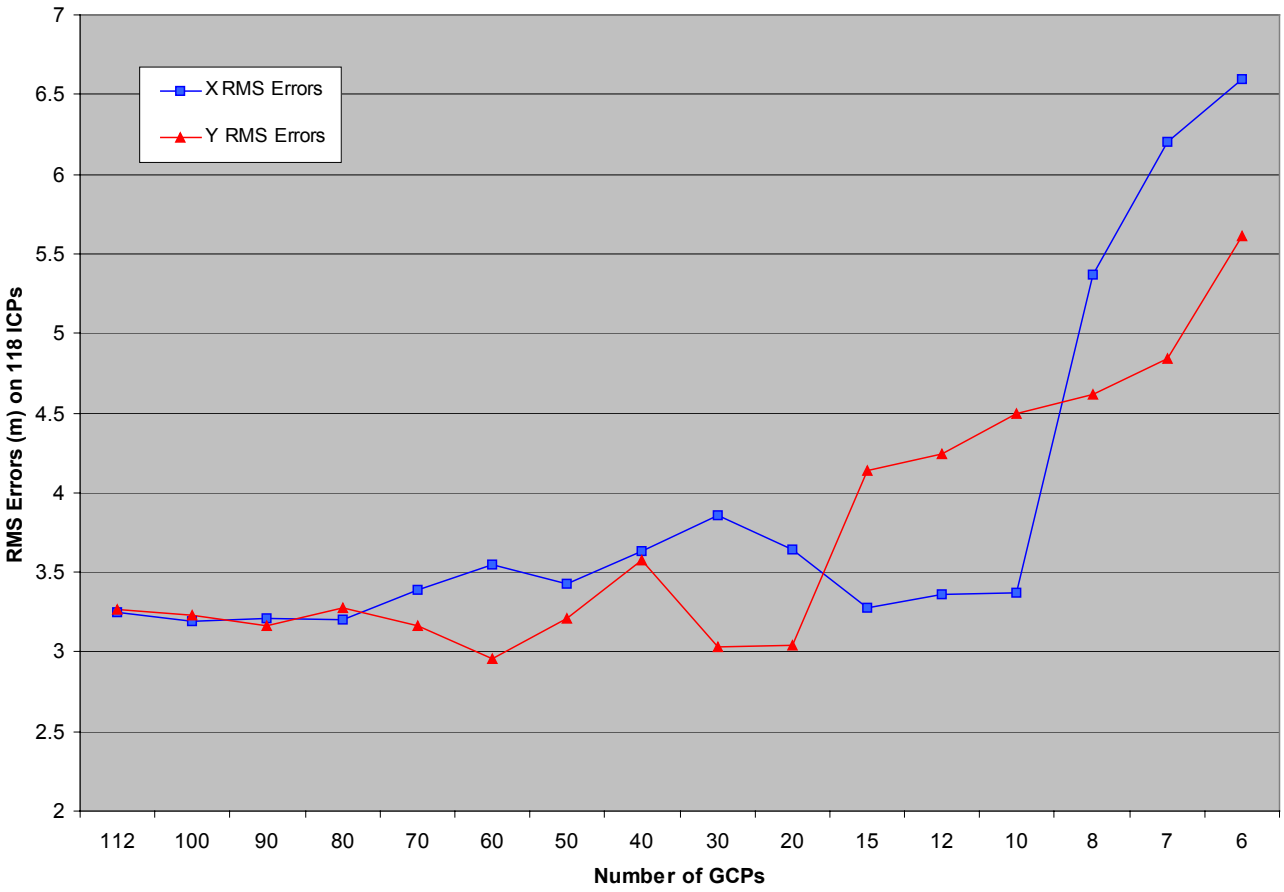

Figure 1. Root mean square (RMS) errors (in metres) on 118 1-m accurate ICPs from the least-square bundle adjustment computed with GCPs varying from 112 to 6 for the Dresden study site.

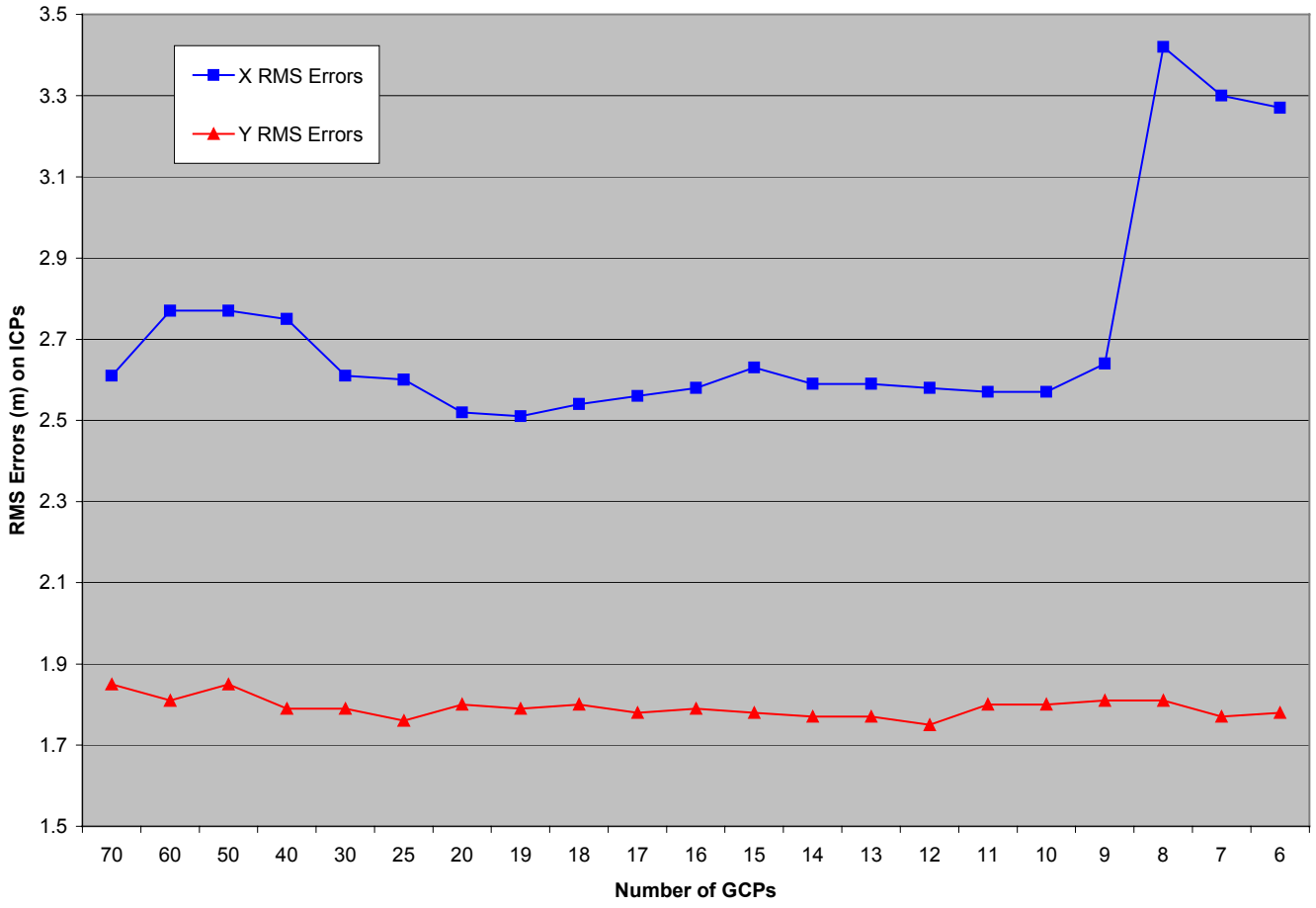

Figure 2. Root mean square (RMS) errors (in metres) on 1-m accurate ICPs from the least-square bundle adjustment computed with GCPs varying from 70 to 6 for the Dresden study site.

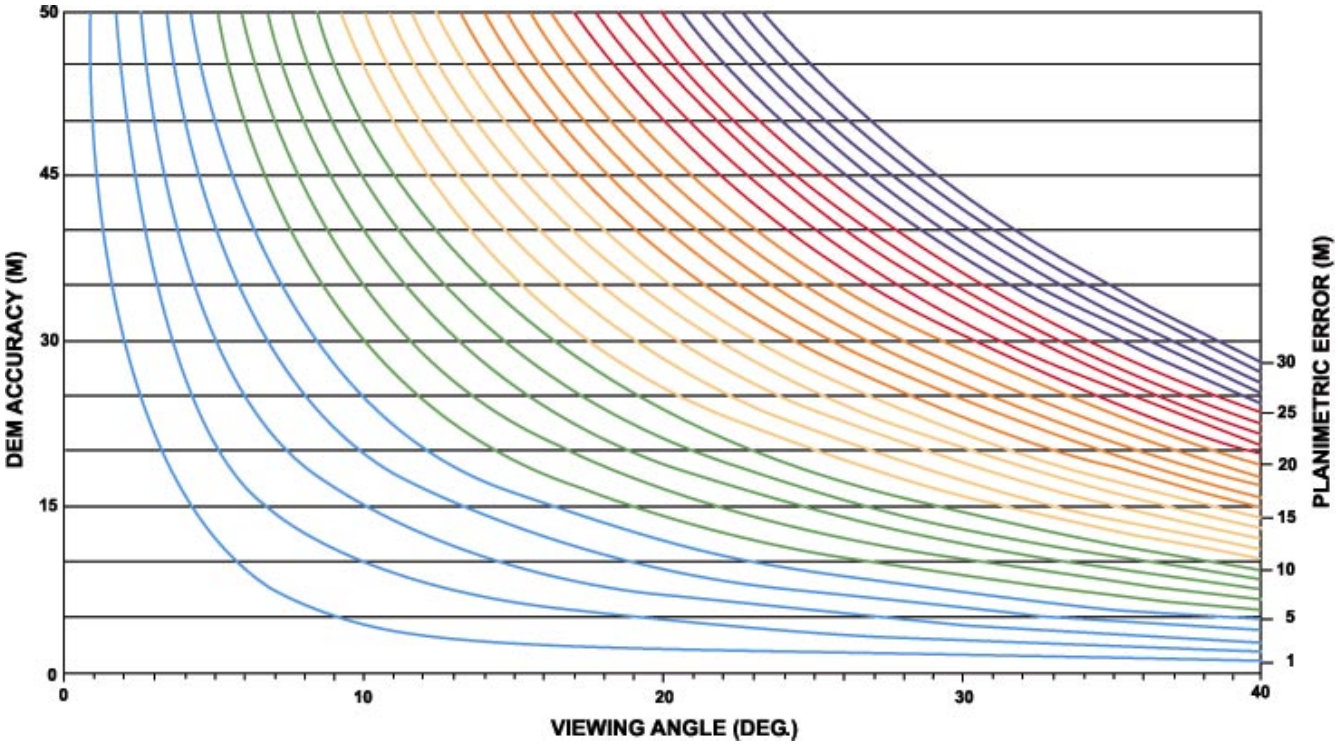

Figure 3: Relationship between the acquisition viewing angle (in degrees), the elevation error (in metres) and the planimetric error on the ortho-image (in metres).

Figure 4. Sub-area of the Beauport_A ortho-image (1-m pixel spacing, 512 pixels 512 lines) at the top, and of the Beauport ortho-photo (1-m pixel spacing, 512 pixels by 512 lines) at the bottom, with 1:25,000 3-m accurate vector lines overlaid.

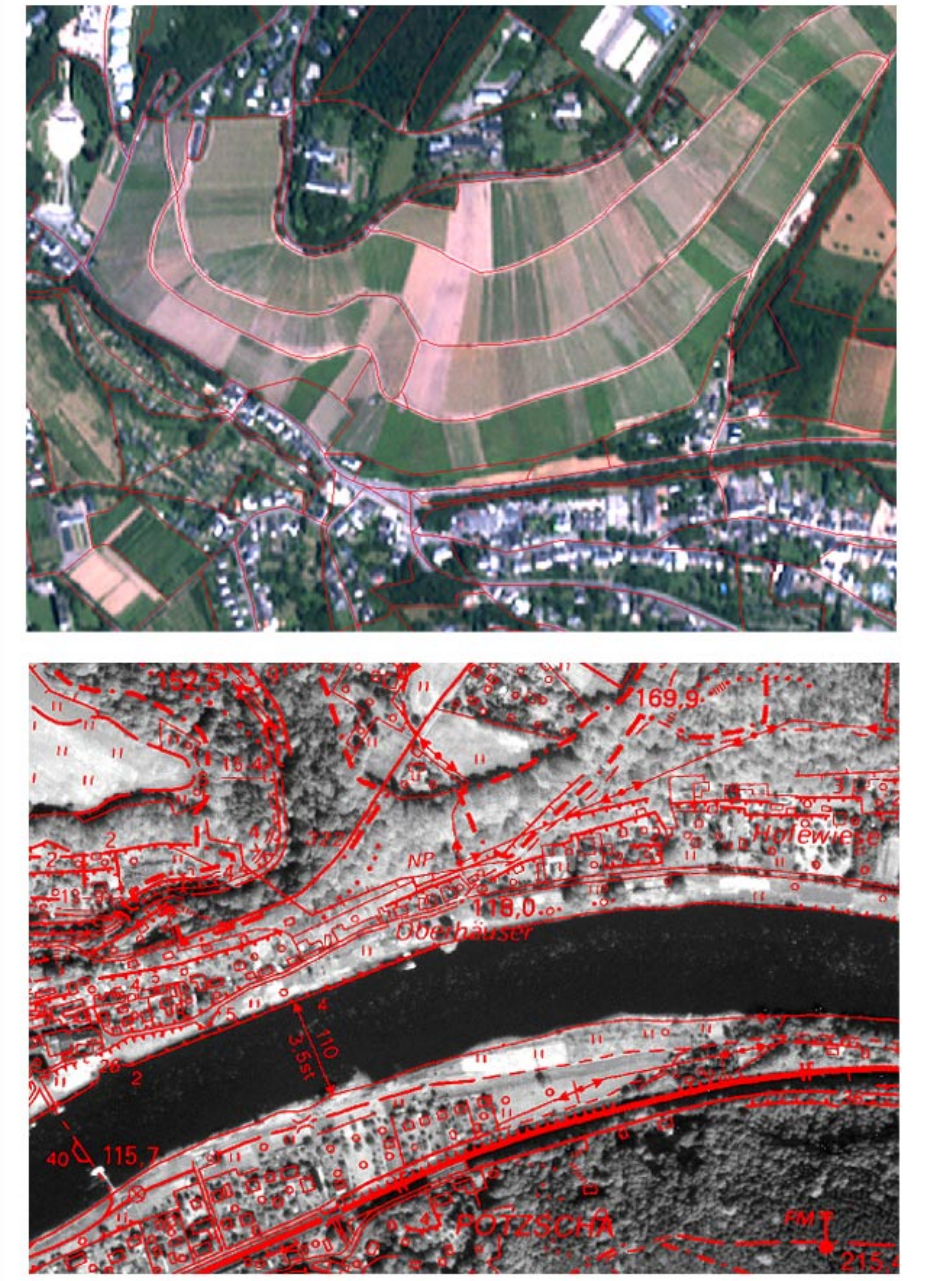

Figure 5. Sub-area of the Trier ortho-image (2-m pixel spacing, 640 pixels by 440 lines) at the top, and of the Dresden ortho-image (1-m pixel spacing, 940 pixels by 660 lines) at the bottom, with 2-m accurate vector lines overlaid.

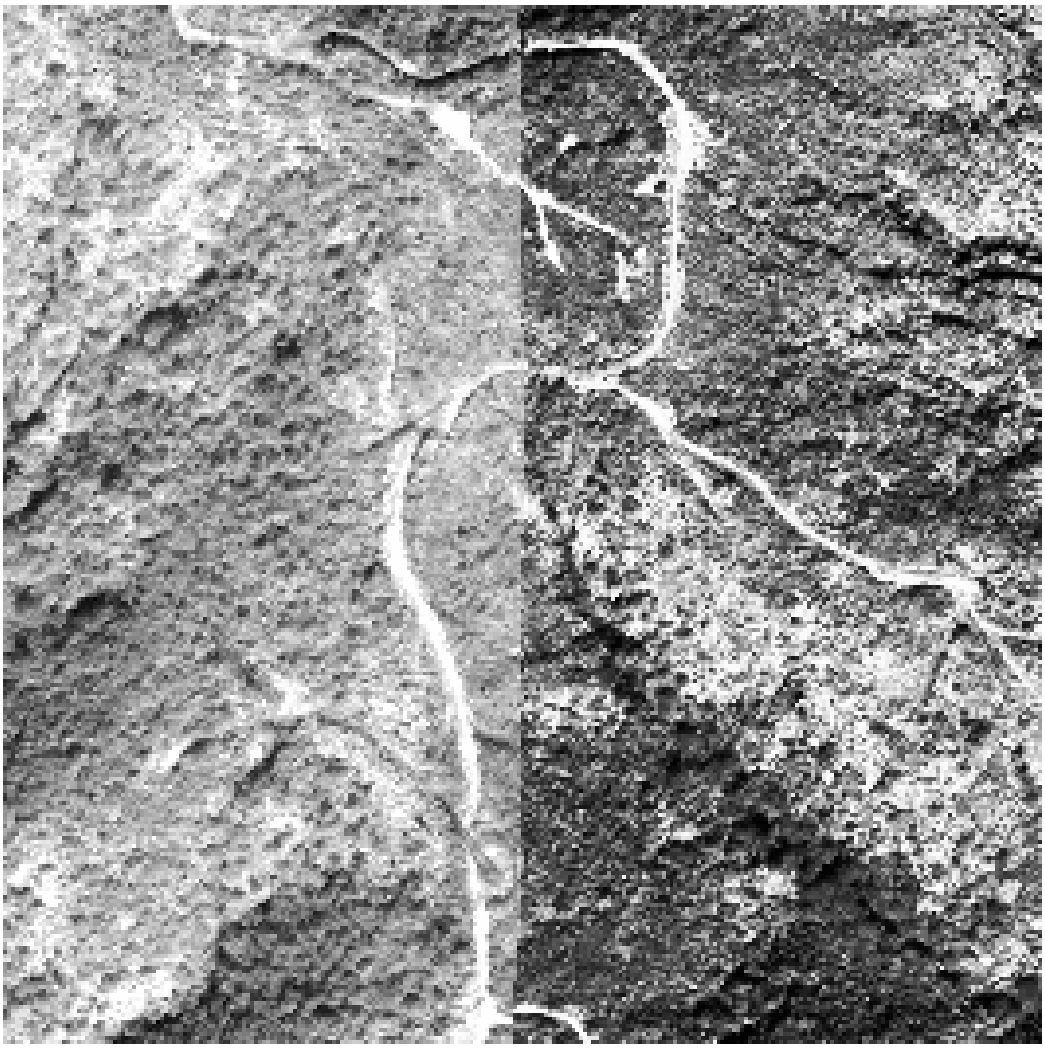

Figure 6. Sub-area (1-m pixel spacing, 512 pixel by 512 lines) of the Caracas_A and _B ortho-mosaic at the image overlap area in the mountains. Radiometric variations between the images were enhanced to show the seed.

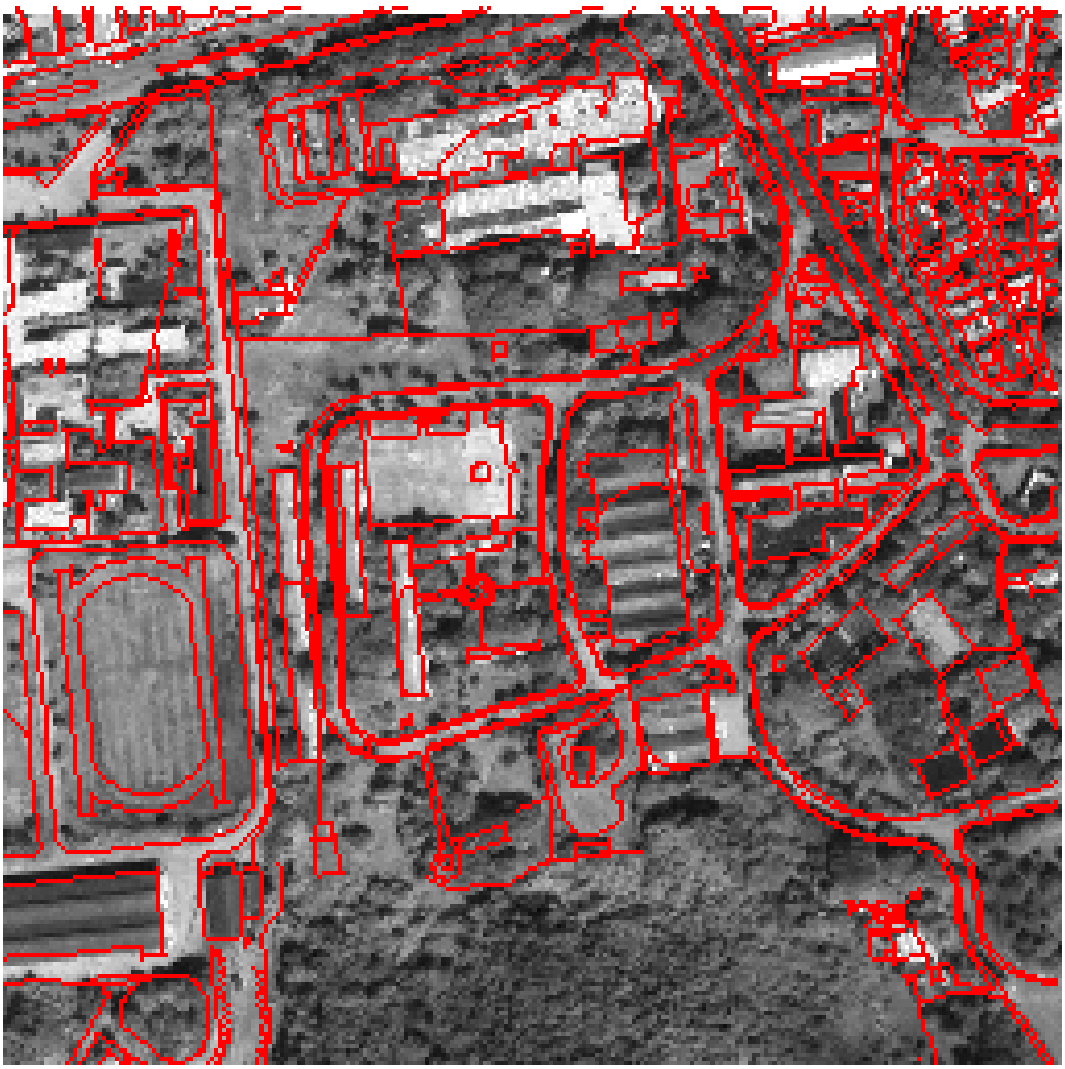

Figure 7. Sub-area (1-m pixel spacing, 512 pixel by 512 lines) of the Caracas_A ortho-image at the coastal area with the 1:1,000 1-m accurate vector lines overlaid.